ETG Turbulence Isotropization

Stefan Tirkas[1]

Hoatian Chen[1]   Gabriele Merlo[2]   Scott Parker[1]

[1]CIPS, University of Colorado, Boulder

[2]University of Texas, Austin

November 9, 2020

University of Colorado **Boulder**

Outline

University of Colorado **Boulder**

Drift Wave Instabilities

- Drift waves are characterized as density, temperature or pressure fluctuations in plasmas.

- Modes relevant to tokamak physics include ion-temperature-gradient modes (ITG), electron-temperature-gradient modes (ETG), and trapped electron modes (TEM).

- Low-frequency drift wave turbulence is largely responsible for the anomalous transport of plasma particles across magnetic field lines (Horton 1999).
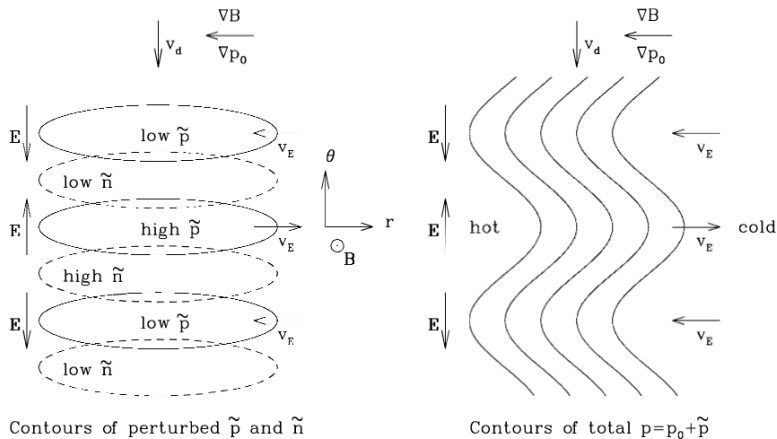
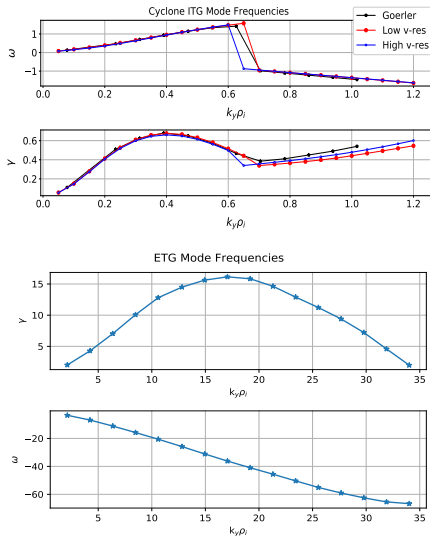University of Colorado **Boulder**

Ion-Temperature-Gradient Mode Growth

Figure: Picture of ITG instability (Beer 1994).
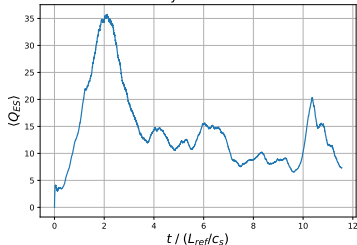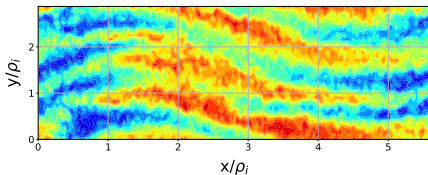
- Successful reproduction of Görler benchmark with kinetic ions and electrons (Görler 2016).

- Conversion of ITG to ETG flux-tube case prior to running non-linear simulations.

ETG "Streamers" in GENE

- ETG turbulence in toroidal gyrokinetic simulations is associated with radially elongated "streamers".

- Multiscale turbulence simulations have shown that streamers dominate electron heat flux and lead to experimental tokamak heat flux values (Howard 2016).

University of Colorado **Boulder**

- Partial differential equation derived from fluid continuity and momentum equations.
- Approximations made that are useful to describing turbulence in tokamak plasmas.
  - Cyclotron motion periods much smaller than time scales that quantities of interest change on (B,Φ,n).
  - Long length scales along $\hat{b}$-direction - $k_{\parallel}/k_{\perp} \equiv \epsilon \ll 1$.
  - Quasi-neutrality of particle densities is enforced.
  - Adiabatic ions.
  - Isothermal equation of state, with $\delta P_e = \delta n_e T_e$ ($\delta T_e = 0$).
- Shown to cause isotropic behavior for long wavelength modes as well as an inverse energy-cascade (Hasegawa 1978).

University of Colorado **Boulder**

Hasegawa-Mima Equations

We start with the fluid continuity and momentum equations with $\tau = T_e/T_i$, where we have already taken the approximations discussed on the previous slide:

$$\frac{\partial n_e}{\partial t} + \nabla \cdot (n_e \vec{v}_e) = 0, \tag{1}$$

$$m_e \frac{d\vec{v}_e}{dt} = (1 + \tau) e \nabla \delta\Phi - \frac{e}{c} \vec{v}_e \times \vec{B} - \frac{\nabla P_e}{n_e}. \tag{2}$$

Then $\vec{v}_e$ is solved for using (2) and plugged into (1), dropping terms higher order than ϵ to get a final PDE describing the evolution of $\delta\Phi$. The derivation is carried out in the Appendix A.

University of Colorado **Boulder**

Hasegawa-Mima Equations

Taking a standard electron dynamic normalization,

$$
\Phi = \frac{e\delta\Phi}{T_i}, \; -\frac{1}{r_n} = \frac{\partial_x n_e}{n_e}, \; -\frac{1}{r_t} = \frac{\partial_x T_e}{T_e}, \; \eta_e = \frac{r_n}{r_t},
$$
$$
\rho_e = \sqrt{\frac{\tau m_e}{m_i}}\rho_i, \; \vec{x} = \frac{\vec{x}}{\rho_e}, \; t = \frac{\rho_e}{r_n}\omega_{ce}t, \tag{3}
$$

and plugging into (10) gives the form of the H-M ETG model,

$$
-(1 - \frac{1+\tau}{2\tau}\nabla_\perp^2)\partial_t\Phi + \frac{1+\tau}{2\tau}\frac{r_n^2}{\rho_e^2}\partial_t^{-1}\nabla_\parallel^2\Phi + \frac{(1+\tau)(1+\eta_e)}{4\tau}\partial_y\nabla_\perp^2\Phi
$$
$$
+ \frac{1+\eta_e}{2\tau}\partial_y\Phi + \frac{(1+\tau)^2}{\tau^2}\frac{r_n}{4\rho_e}(\hat{b}\times\nabla_\perp\Phi\cdot\nabla_\perp)\nabla_\perp^2\Phi = 0 \,. \tag{4}
$$

University of Colorado **Boulder**

We drop the higher order parallel gradient term and simplify the bracketed expression for a 2-D slab geometry to find the final form,

$$
\partial_t[\Phi - \frac{1+\tau}{2\tau}\zeta] = \frac{(1+\tau)(1+\eta_e)}{4\tau}\zeta_y + \frac{1+\eta_e}{2\tau}\Phi_y
$$
$$
+ \frac{(1+\tau)^2}{\tau}\frac{r_n}{4\rho_e}[\Phi_x\zeta_y - \zeta_x\Phi_y],
$$

(5)

where $\zeta = \nabla^2\Phi$ and x, y subscripts denote partial derivatives. The non-linear terms lead to rotation in k-space and eventually isotropization.

University of Colorado **Boulder**

Pseudo-Spectral Solver

- Equation (6) is solved numerically using the pseudo-spectral method.
  - Fourier transform the equation and get $\zeta = -(k_x^2 + k_y^2)\Phi$.
  - Inverse Fourier transform $\zeta_{x,y}$ and $\Phi_{x,y}$ back into real space.
  - Calculate the non-linear products between ζ and Φ in real space and then Fourier transform the products so they can be added to the other terms in Fourier space.
  - Time advance Φ discretely.

- Time advancement is done using the 4th order Runge-Kutta method.

- The pseudo-spectral method requires de-aliasing of modes due to non-linear terms. This is explored in Appendix B.

University of Colorado **Boulder**

ETG H-M Results
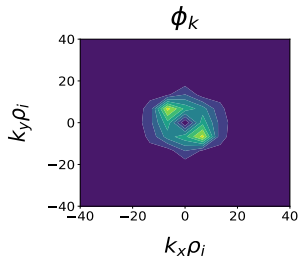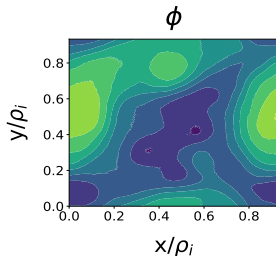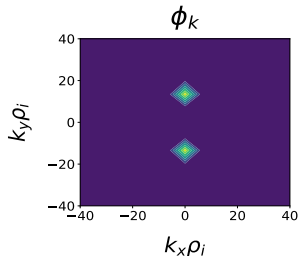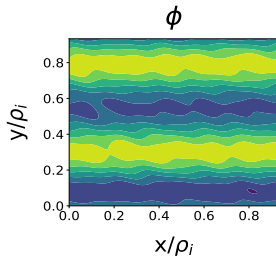
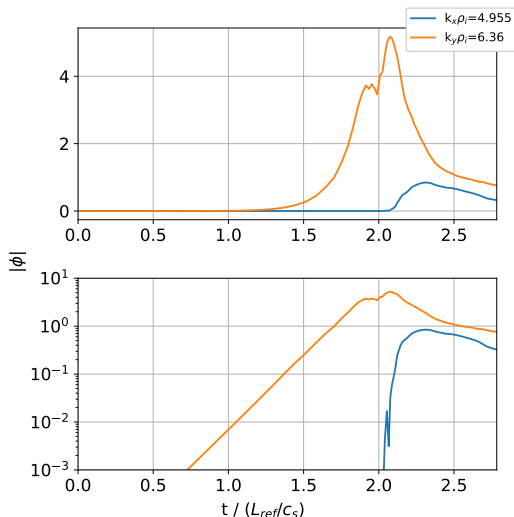- Results of H-M code. Initial condition (above) isotropizes at late time (below).
- Parameters:
  - $\tau = 1$
  - $\eta_e = 3$
  - $r_n/\rho_i = 500$

University of Colorado **Boulder**

GENE ETG Streamer Test
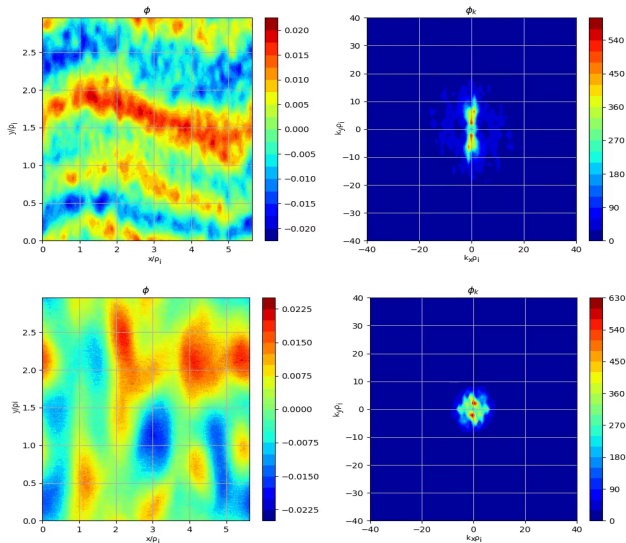
- Test of GENE saturated ETG results into H-M code. Initial condition (above) isotropizes at late time (below).
- Inverse energy cascade observed as well.

University of Colorado **Boulder**

Zonal Flow Excitation

- Zonal flow can be spontaneously excited by intermediate-scale ETG turbulence in tokamak geometries - $k_\perp \rho_e \ll 1 \ll k_\perp \rho_i$.

- Plan to carry out large-scale ETG simulations with GENE to compare to theory of zonal flow excitation by ETG modes.

University of Colorado **Boulder**

Four-Wave Weak Turbulence Model

$$(\partial_t + \gamma_z(1 + d_z k_z^2 \rho_e^2))\chi_z A_z = \sqrt{\pi/2} W k_z^3 \rho_e^3 (A_+ A_0^* a_n^* - A_-^* A_0 a_n),$$

$$[\partial_t + i\Delta - \gamma_s]A_+ = -W k_z \rho_e A_z A_0 / \sqrt{2\pi},$$

$$[\partial_t + i\Delta - \gamma_s]A_- = W k_z \rho_e A_z^* A_0 / \sqrt{2\pi},$$

$$[\partial_t - \gamma_n]A_0 = -W k_z \rho_e (A_z A_- - A_z^* A_+) / \sqrt{2\pi},$$

$$(\partial_t - 2\gamma_n)|A_0|^2 = (2\gamma_s - \partial_t)(|A_+|^2 + |A_-|^2)$$

- $A_z \equiv$ Zonal Flow Amp.
- $A_\pm \equiv$ Sideband Amp.'s
- $A_0 \equiv$ ETG Pump Wave
- $a_n \equiv$ Parallel coupling fn.

- $W \equiv$ Bandwidth
- $\gamma_{z,n,s} \equiv$ Growth rates
- $\chi_z \equiv$ Susceptibility
- $k_z \equiv$ radial k

We break up (2) into parallel and perpendicular components by taking a dot product with $\hat{b}$ to find,

$$\frac{d\vec{v}_{e,\parallel}}{dt} = (1 + \tau)\frac{e}{m_e}\partial_t^{-1}\nabla_{\parallel}\delta\Phi \Rightarrow v_{\parallel} \simeq (1 + \tau)\frac{k_{\parallel}e\delta\Phi}{m_e\omega}, \qquad (6)$$

$$\frac{d\vec{v}_{e,\perp}}{dt} = (1 + \tau)\frac{e}{m_e}\nabla_{\perp}\delta\Phi - \omega_{c,e}\vec{v}_{e,\perp} - \frac{\hat{b} \times \nabla P_e}{m_e n_e} . \qquad (7)$$

University of Colorado **Boulder**

Then we can split up $\vec{v}_e$ by ordering

$$\vec{v}_{e,0} = \vec{v}_{\parallel} + \vec{v}_{\perp,0} = \vec{v}_{\parallel} + (1+\tau)\,\vec{v}_E + \vec{v}_D,$$

$$\vec{v}_{e,1} = \vec{v}_{\perp,1} = -\frac{1}{\omega_{c,e}}(\partial_t + \vec{v}_{e,0}\cdot\nabla)(\hat{b}\times\vec{v}_{e,0})$$

$$\simeq \frac{e(1+\tau)}{m_e\omega_{c,e}^2}\partial_t\nabla_\perp\delta\Phi - [\frac{\vec{b}\times\nabla P_e}{n_e}\cdot\nabla_\perp]\frac{e(1+\tau)}{m_e^2\omega_{c,e}^3}\nabla_\perp\delta\Phi \tag{8}$$

$$+ \frac{e^2(1+\tau)^2}{m_e^2\omega_{c,e}^3}[\hat{b}\times\nabla_\perp\delta\Phi\cdot\nabla_\perp]\nabla_\perp\delta\Phi\,.$$

University of Colorado **Boulder**

Appendix A: H-M Fluid Model

Now, with incompressibility and to lowest order, $\nabla \cdot \vec{v}_{e,0,\perp} = 0$ and so (1) becomes,

$$\partial_t \delta n_e + n_e \nabla \cdot (v_\parallel + \vec{v}_{e,1}) + \nabla \delta n_e \cdot \vec{v}_D + (1 + \tau)\delta n_e \cdot \vec{v}_E = 0, \qquad (9)$$

and plugging in $\delta n_e = \delta n_i$, we find that to order ϵ,

$$- n_e \partial_t \frac{e\delta\Phi}{T_i} + n_e(1+\tau)\frac{e}{m_e}\partial_t^{-1}\nabla_\parallel^2 \delta\Phi + \frac{en_e(1+\tau)}{m_e\omega_{c,e}^2}\partial_t \nabla_\perp^2 \delta\Phi$$

$$- \frac{e(1+\tau)}{m_e^2\omega_{c,e}^3}[\hat{b} \times \nabla P_e \cdot \nabla_\perp]\nabla_\perp^2 \delta\Phi + \frac{e^2 n_e(1+\tau)^2}{m_e^2\omega_{c,e}^3}[\hat{b} \times \nabla_\perp\delta\Phi \cdot \nabla_\perp]\nabla_\perp^2 \delta\Phi$$

$$+ \nabla_\perp \frac{e\delta\Phi}{T_i} \cdot \frac{\hat{b} \times \nabla P_e}{m_e\omega_{c,e}} + \frac{e(1+\tau)}{m_e\omega_{c,e}}\nabla n_e \cdot \hat{b} \times \nabla\Phi = 0 .$$

$$(10)$$

Appendix B: Pseudo-Spectral De-Aliasing

Our Fourier transforms go as $e^{-ik_j z_n}$ with wave-vectors $k_j = 2\pi j/N\Delta$, and grid points $x_n = n\Delta$, where $j = -N/2, ..., N/2$, and $n = 0, ..., N - 1$. So the final form for our modes is $e^{-2\pi i n j/N}$. If we consider non-linear terms then we can take $j' = j + lN$ with $l = ..., -1, 0, 1, ...$, which will take j out of the range well-resolved by the Fourier transform. The extra term $e^{-2\pi i l n} = 1$ results in the same values at our grid points. This means non-linear terms can lead to biasing of lower, well-resolved modes via higher modes. To de-alias we choose the truncation (or $2/3$) rule which says to zero out modes between $[-N/2, -K]$ and $[K, N/2]$. That way if we have two modes $|j + k| > N/2$ the final mode is resolved as $j + k - N$ which must be $< -K$ to be zeroed out. Since the largest allowed option is K for each mode, we get $2K - N < -K \Rightarrow K < N/3$. This means keeping $2/3$ of the original modes when considering non-linear terms.